Biochemical Compounds
ISSN 2052-9341 | Volume 5 | Article 4

HOAJ
Herbert Open Access Journals

Special Section | Biomolecules | Original Research Open Access

Melting behavior of pseudoknots containing adjacent GC and AT rich domains

Calliste Reiling-Steffensmeier, Mikenzie Nordeen and Luis A. Marky*

*Correspondence: lmarky@unmc.edu

Department of Pharmaceutical Sciences, College of Pharmacy, University of Nebraska Medical Center, 986025 Nebraska Medical Center, Omaha, NE 68198-6025, United States.

Abstract

Background: Z-DNA is very important in transcription when RNA polymerase transcribes and Z-DNA is formed on the 5' end following the polymerase. Pseudoknots have also been found to play important roles in the biology of RNA, such as the expression of genes and in the overall tertiary structure of RNA molecules.

Methods: A combination of UV and circular dichroism (CD) spectroscopies and differential scanning calorimetry (DSC) were used to investigate the UV/CD spectral characteristics and the unfolding thermodynamics of two DNA pseudoknots with the following sequences: d(CGCGCGT_5GAAATTCCGCGCGT_5GAATTTC) (***CG-PsK***) and d(GCGCGCT_5CAAATT-GGCGCGCT_5CAATTTG) (***GC-PsK***), where "T_5" are loops of five thymines, along with, two control self-complementary duplexes, $d(CG)_3$ (***Du-CG***) and $d(GC)_3$ (***Du-GC***).

Results: The UV/DSC melts showed sequential biphasic (***CG-PsK***) and triphasic (***GC-PsK***) transitions, with T_Ms independent of the strand concentration. Their DSC unfolding took place in two independent parts, the unfolding of the AT rich stem followed by the GC rich stem. ***CG-PsK***'s thermodynamic profiles under both salt conditions were similar, while the stability and the folding enthalpy were lower in this salt range for ***GC-PsK***. The CD spectrum showed the $d(CG)_3$ portion of the stem of ***CG-PsK*** flips into a left handed helix in high salt conditions that could be affecting the loop/stem interplay, yielding a higher folding enthalpy relative to ***GC-PsK***.

Conclusions: Each pseudoknot formed intramolecularly with sequential transitions corresponding to the associated AT and GC rich melting domains. The placement of d(CG) in ***CG-PsK*** yielded a CD spectra with a partial transition of the full stem to a left-handed helix. The melting behavior of ***CG-PsK*** remained unchanged with the addition of salt, while ***GC-PsK*** was greatly affected due to a more constrained right stem of the pseudoknot. The main reasons for these differences was the melting behavior of the AT rich motif, which is explained in terms of a loop/stem interplay within ***GC-PsK***, hydration differences of their dA•dT base pairs, and/or the conversion of ***CG-PsK*** to a partial left handed helix. This conversion could be helping to stabilize this pseudoknot allowing the right stem to be less constrained at 5 M NaCl.

Keywords: Intramolecular DNA structures, pseudoknots, thermodynamics, differential scanning calorimetry, circular dichroism, left-handed DNA

Introduction

Z-DNA is a rare left-handed double-helix which requires alternating GC rich sequences [1,2]. It is more elongated and narrow than both B and A-DNA and has a zigzag backbone due to the alternate stacking of bases in *anti* and *syn*-conformations. Due to the electrostatic repulsion of the phosphates, Z-DNA is more favorable at high salt concentrations by reducing this effect [3,4]. However, these high salt conditions are not present *in vivo*, but cytosine methylation, spermine, and spermidine can also help to stabilize the Z-conformation [5,6]. It has been found that Z-DNA is mainly present when DNA is undergoing negative supercoiling and also during transcription [7,8]. For

doi: 10.7243/2052-9341-5-4

example, when the RNA polymerase binds to the DNA the Z-conformation is formed behind the polymerase due to the negative torsional constrain. This is because the polymerase is not rotating while it's transcribing [9,10].

Z-DNA has been found in both prokaryotic and eukaryotic systems. In prokaryotes, B-DNA is transformed to Z-DNA to avoid undesired methylation [11]. Also in *E. coli,* Z-DNA can form which is regulated by transcription and enhanced by inactivating topoisomerase through mutations [12,13]. Z-DNA in eukaryotes is highly immunogenic, both polyclonal and monoclonal antibodies can bind to this conformation [14,15]. In murine cells it was shown that three transcription-dependent Z-DNA-forming segments were identified in the 5′ region of a gene with two of them near promoters [16,17]. Studies on Z-DNA have shown that the majority forms behind a moving RNA polymerase and is stabilized by the negative supercoiling generated by DNA transcription [18,19].

Pseudoknots are also very important in biological systems. Their functional roles include, but are not limited to, the catalytic cores of various ribozymes, self-splicing introns, riboswitches, and ribosomal frameshifting [20-24]. Pseudoknots are perhaps the foundation of the large number of structures that RNA molecules undertake due to its intramolecular nature. It has also been found that RNA with rich CG regions is able to adopt the Z-conformation [25,26]. It could be possible that pseudoknots with CG rich stems can flip into the Z-conformation aiding in the control of gene expression. Riboswitches are often found near ribosomal binding sites and formation of pseudoknots can stop the ribosome from binding by blocking access to the RBS in the mRNA [27,28], so there could be a similar mechanism as seen with transcription. It is of interest to see whether or not the inclusion of a $d(CG)_3$ segment can form a left-handed conformation imbedded in a DNA pseudoknot and how this affects the overall melting behavior of the pseudoknot.

In this work, we have designed DNA pseudoknots containing adjacent GC and AT rich domains along with two control duplexes, one being $d(CG)_3$ and the other $d(GC)_3$ to mimic the GC rich domains of each pseudoknot. We used temperature-dependent unfolding techniques (UV, CD and DSC), to test the conformational rearrangements within the pseudoknots and measured the associated energetics that accompanies their melting behavior.

Materials and methods

Materials

All oligonucleotides were synthesized by Integrated DNA Technologies (IDT) (Coralville, IA), HPLC purified, and desalted by column chromatography using G-10 Sephadex exclusion chromatography. The sequences of oligonucleotides used in this work and their designation are shown in **Figure 1**. The concentrations of the oligomer solutions were determined at 260 nm and 90°C or 100°C using an Aviv Spectrophotometer Model 14DS UV-Vis and the molar extinction coefficients:

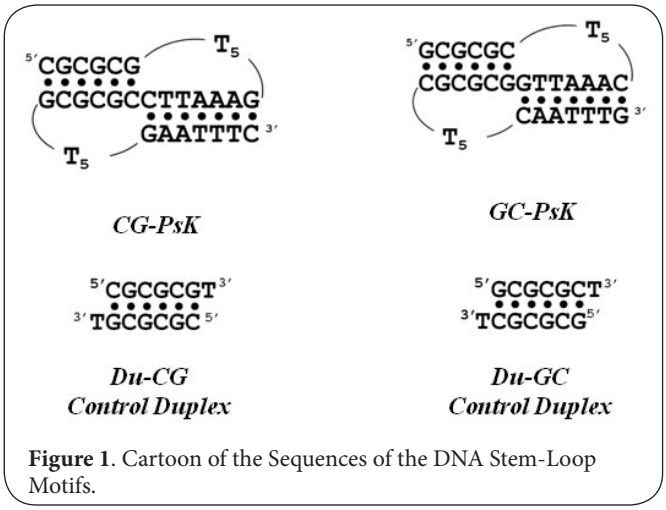

Figure 1. Cartoon of the Sequences of the DNA Stem-Loop Motifs.

326.5 mM^{-1} cm^{-1} (***CG-PsK***), 320.6 mM^{-1} cm^{-1} (***GC-PsK***), 60.0 mM^{-1} cm^{-1}(***Du-CG***), 59.8 mM^{-1} cm^{-1}(***Du-GC***). These values were obtained by extrapolation of the tabulated values for dimers and monomeric bases [29] at 25°C to 90°C or 100°C using procedures reported previously [30,31]. Inorganic salts from Sigma were reagent grade, and used without further purification. Measurements were made in appropriate buffer solutions: 10 mM sodium phosphate (NaPi), 1 M NaCl or 5 M NaCl at pH 7.0. All oligonucleotide solutions were prepared by dissolving the dry and desalted ODNs in buffer.

Temperature-Dependent UV Spectroscopy (UV)

Absorbance versus temperature profiles were measured at 260, 268, and 275 nm with a thermoelectrically controlled Aviv Spectrophotometer Model 14DS UV-Vis (Lakewood, NJ). The temperature was scanned at a heating rate of approximately 0.6 °C/min, and shape analysis of the melting curves yielded transition temperatures, T_Ms [30]. The transition molecularity for the unfolding of a particular complex was obtained by monitoring T_M as a function of the strand concentration. Intramolecular complexes show a T_M-independence on strand concentration, while the T_M of intermolecular complexes does depend on strand concentration [31].

Differential scanning calorimetry (DSC)

The total heat required for the unfolding of each oligonucleotide, in appropriate buffer conditions, was measured with a VP-DSC differential scanning calorimeter from Malvern (Northampton, MA). T_Ms and standard thermodynamic profiles are obtained from these thermograms, ΔC_p as a function of temperature, using the following relationships [30,31]: $\Delta H_{cal} = \int \Delta C_p(T) dT$; $\Delta S_{cal} = \int \Delta C_p(T)/T dT$, and the Gibbs equation, $\Delta G°_{(T)} = \Delta H_{cal} - T\Delta S_{cal}$; where ΔC_p is the anomalous heat capacity of the ODN solution during the unfolding process, ΔH_{cal} and ΔS_{cal} are the unfolding enthalpy and entropy, respectively, assumed to be temperature-independent. $\Delta G°_{(T)}$ is the free energy at temperature T, 20°C.

doi: 10.7243/2052-9341-5-4

Circular dichroism (CD)

All CD spectra were obtained with an Aviv Circular Dichroism Model 202SF spectrometer (Lakewood, NJ) equipped with a peltier temperature control system. These CD spectra were taken from 320 nm to 220 nm in 1 nm increments with an averaging time of 3 seconds using 0.1 cm free-strained quartz (Suprasil) cuvettes. The reported spectra correspond to the average of at least two scans. The particular conformation of each pseudoknot or duplex (10 mM NaPi with 1 M or 5 M NaCl) was determined from inspection of their CD spectra at 2 or 25°C, where the oligos were completely folded.

Results and discussion

Temperature-induced UV melting of Pseudoknots

Figure 2 shows typical UV melting curves at 268 nm for the helix-coil transition of each pseudoknot and control duplexes in 1 M and 5 M NaCl. Their sigmoidal behavior is characteristic of the temperature-induced unfolding of nucleic acid helices. In 1 M salt, ***CG-PsK*** had two transitions with T_Ms and ΔH_{vH}s of 44.6°C, 64 kcal/mol and 76.6°C, 44 kcal/mol, respectively. ***GC-PsK*** also had two transitions but the first one was broad while the second one was well defined, T_M = 82.2°C and ΔH_{vH} = 48 kcal/mol. Similar results were obtained for ***CG-PsK*** in 5 M salt, two transitions with T_Ms and ΔH_{vH}s of 41.7°C, 64 kcal/mol and 76.0°C, 45 kcal/mol, respectively. ***GC-PsK*** again had one defined transition, with a T_M of 75.7°C and ΔH_{vH} of 38 kcal/mol. These UV melting parameters, based on the measured T_Ms, indicate that the initial transition(s) of the pseudoknots correspond to the AT rich segment of their stem, while the last transition corresponds to the melting of their GC rich domain. This was in qualitative agreement with the UV melting parameters of the control duplexes containing 6 dG•dC base pairs each, which exhibited one transition with T_Ms and ΔH_{vH}s in 1 M salt: 61.4°C, 51 kcal/mol (***Du-CG***) and 62.8°C, 53 kcal/mol (***Du-GC***). However, the increase in the salt to 5 M yielded decreases in both T_M and ΔH_{vH}: 53.6°C, 44 kcal/mol (***Du-CG***) and 52.1°C, 44 kcal/mol (***Du-CG***). The higher thermal stability of the pseudoknots was due to the fact that these molecules fold/unfold intramolecularly while the folding/unfolding transitions of the control duplexes were bimolecular.

Based on both the shape of the pseudoknot UV melts and the melting data of their last transitions, the main observations are: ***GC-PsK*** was more stable in 1 M salt while their stability was similar in 5 M salt. A similar trend was observed with the control duplexes i.e., ***Du-GC*** was more stable in 1 M whereas similar stability for both duplexes was obtained in 5 M. The overall observation was consistent with their number of base pair stacks, three CG/GC & two GC/CG (***CG-PsK***) and two CG/GC & three GC/CG (***GC-PsK***). On the other hand, it is difficult to discuss the melting behavior of the AT rich motif of these pseudoknots, which differ mainly by two base pair stacks i.e., two CT/GA in ***CG-PsK*** are replaced for two CA/TG in ***GC-PsK***, which may interact differently with the adjacent loop of 5 thymines. However, the DSC results of a later section will show some light on the melting behavior of this AT rich motif of the pseudoknots.

Circular Dichroism (CD)

The CD spectra obtained in both 1 M and 5 M NaCl for all four molecules are shown in **Figure 3**. The CD spectra of ***CG-PsK***, ***GC-PsK***, ***Du-CG***, and ***Du-GC*** in 1 M NaCl showed two bands with similar intensities and areas, and with minimums around 250 nm and maximums at 275 nm, which are characteristic of a nucleic acid in the "B" conformation [**32**]. In 5 M salt, the positive band of the ***CG-PsK*** spectrum (**Figure 3A**) showed a slight shift to 272 nm; however, an additional band with a minimum at 293 nm was observed. The ***GC-PSK*** spectrum

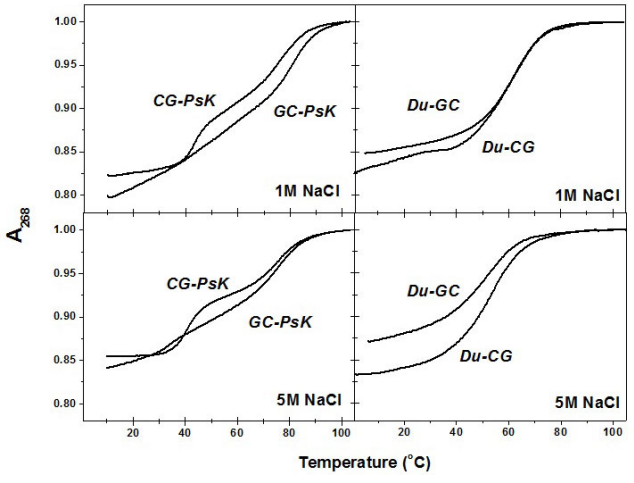

Figure 2. UV Melting Curves.
All experiments were performed in 10 mM NaPi with 1 M or 5 M NaCl buffer pH 7.0 at concentrations ranging from 27-65 μM; T_M (±0.5°C).

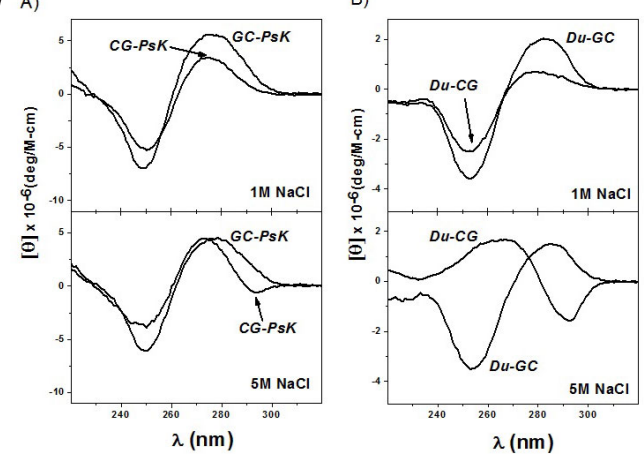

Figure 3. CD Spectra.
All experiments were performed in 10 mM NaPi with 1 M or 5 M NaCl buffer pH 7.0. Spectra were obtained from 320 nm to 220 nm with concentrations ranging from 27-65 μM.

doi: 10.7243/2052-9341-5-4

remained the same. The CD spectra of the duplexes showed a trend similar to the pseudoknots in 5 M salt; however, the spectra of ***Du-CG*** was completely flipped with a minimum at 294 nm and a maximum at 265 nm, indicating a complete left-handed helix was formed [33]. The CD spectrum of ***Du-GC*** remained the same i.e., ***Du-GC*** remained in the B-conformation. The additional band in the ***CG-PsK*** spectrum at 5 M was therefore due to a partial flip into a left-handed helix, which was confirmed by the addition of the spectra of ***Du-GC*** and ***Du-CG*** at 5 M salt that produced a similar dip in the spectra at 294 nm (data not shown). This exercise was simulating the right-handed stem (GAAATTC/GAATTTC) and left-handed stems (CGCGCG/GCGCGC) of ***CG-PsK***. This observation indicated that at this high salt concentration the 13 base pair stem of ***CG-PsK*** is a mixture of both a right-handed (right stem) and a left-handed (left stem) helix.

Unfolding Thermodynamics Obtained From Differential Scanning Calorimetry (DSC)

The DSC thermograms of each pseudoknot and control duplex are shown in **Figure 4** and standard thermodynamic profiles for the folding of each molecule are shown in **Table 1**. The T_Ms were similar to what was obtained by UV melts for each pseudoknot. ***CG-PsK*** in 1 M NaCl had a ΔT_M of 1.3 and 0.3°C for the first and second transition, respectively, and in 5 M a ΔT_M of 0.6 and 1°C. ***GC-PsK*** in 1 M NaCl had a ΔT_M of 0.2°C for the last transition and in 5 M a ΔT_M of 0.7°C. These small differences verified the intramolecular formation of these two pseudoknots in both salt conditions due to the T_M being independent of strand concentration, i.e., we used ten-fold higher concentration in the DSC experiments. The duplexes showed higher T_Ms in both salt conditions. ***Du-CG*** showed a ΔT_M of 3.1 and 1.0°C in 1 and 5 M NaCl, respectively. ***Du-GC*** had a ΔT_M of 4.3 and 2.7°C in 1 and 5 M NaCl, respectively. This indicated the intermolecular formation of the control duplexes due to T_M dependence on strand concentration. Overall, the favorable folding of each pseudoknot, negative $\Delta G°$, took place through the typical favorable enthalpy-unfavorable entropy compensation. Favorable enthalpy contributions correspond to the energy gained by the formation of base pairs and base pair stacking interactions, while unfavorable entropy contributions correspond to the higher ordered state of the helical state of each molecule and the putative uptake of ions and water molecules [34-37]. In 1 M salt concentration, $\Delta G°$s of -11.1 kcal/mol (***CG-PsK***) and -12.2 kcal/mol (***GC-PsK***) were obtained, which were driven by favorable folding enthalpies of -86.8 kcal/mol (***CG-PsK***) and -78.8 kcal/mol (***GC-PsK***), respectively. These folding enthalpies were lower than the ones obtained from nearest-neighbor parameters (-105.8 and -105.6 kcal/mol, respectively) [38] in similar salt concentrations and using the full sequence of the pseudoknot stems. This may be explained in terms of the thymine loops that are somewhat short and constrained producing a reduction on the base pair stacking in the stem, consistent with previous results of pseudoknots with different loop lengths [39]. The increase in

Table 1. Thermodynamic Profiles for the Folding of Pseudoknots and Control Duplexes.

[NaCl]	Transition	T_M (°C)	ΔH_{cal} (kcal/mol)	$\Delta G°_{20}$ (kcal/mol)	$T\Delta S$ (kcal/mol)
		CG-PsK			
1 M	1st	43.0	-33	-2.4	-30.6
	2nd	76.3	-54	-8.7	-45.3
	Total		-87	-11.1	-75.9
5 M	1st	42.3	-35	-2.5	-32.5
	2nd	75.0	-52	-8.2	-43.8
	Total		-87	-10.7	-76.3
		GC-PsK			
1 M	1st	42.8	-4	-0.3	-3.7
	2nd	60.2	-20	-2.4	-17.6
	3rd	82.0	-55	-9.6	-45.4
	Total		-79	-12.3	-66.7
5 M	1st	34.7	-7	-0.3	-6.7
	2nd	52.8	-14	-1.4	-12.6
	3rd	76.4	-48	-7.7	-40.3
	Total		-69	-9.4	-59.5
		Du-CG			
1 M	--	65.4	-51	-6.3	-44.7
5 M	--	55.3	-49	-5.7	-43.3
		Du-GC			
1 M	--	67.1	-51	-7.1	-43.9
5 M	--	54.8	-48	-5.1	-42.9

All experiments were done in 10 mM sodium phosphate buffer with 1 M or 5 M NaCl at pH 7.0. Experimental errors are as follows: T_M (±0.5 °C), ΔH_{cal} (±5 %), $T\Delta S$ (±5%), $\Delta G°_{(20)}$ (±7%).

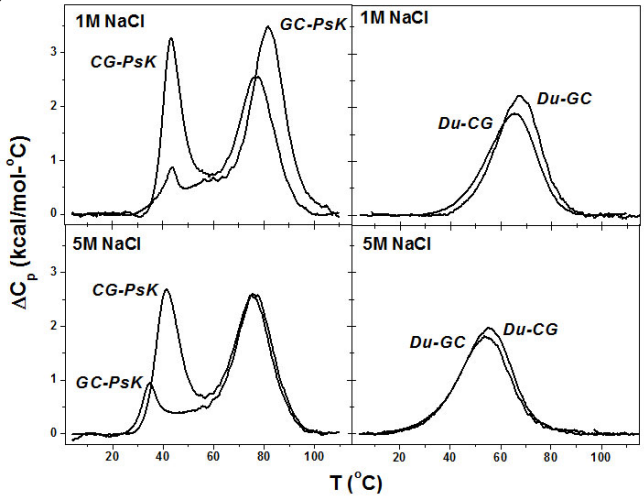

Figure 4. DSC Unfolding Curves.
DSC Experiments were performed in 10 mM NaPi with either 1 M or 5 M NaCl buffer at pH 7.0, with concentrations ranging from 70-240 μM.

doi: 10.7243/2052-9341-5-4

salt concentration to 5 M resulted in less favorable Δ*G*° terms (by 0.4 and 2.7 kcal/mol, respectively), which resulted from a similar enthalpy (***CG-PsK***) and less favorable enthalpy (***CG-PsK***), by 10.2 kcal/mol. The unfolding of each pseudoknot took place with distinctive melting profiles. For instance, ***CG-PsK*** unfolded in two transitions while ***GC-PsK*** unfolded in three transitions; the initial transitions correspond to unfolding of the right stem of each pseudoknot (AT rich domain) and the last transition to the unfolding of their left stem (GC rich domain), which was confirmed by the DSC thermograms of the control duplexes, ***Du-CG*** and ***Du-GC***, respectively. One of the goals of this study was to investigate the folding/unfolding thermodynamics of pseudoknots containing a GC rich motif next to an AT rich motif. The GC rich motif (d(CGCGCG)$_2$) of ***CG-PsK*** was capable of forming a left handed helix when the salt is increased from 1 M to 5 M, as described in the CD section. Before describing the thermodynamic melting behavior of pseudoknots in terms of the two different motifs, it is best to compare what is happening between the control duplexes, ***Du-CG*** and ***Du-GC***, which pertain to the GC rich helical domain on the left of the pseudoknots (**Figure 1**). In 1 M salt concentration, Δ*G*°s of -6.7 kcal/mol (***Du-CG***) and -7.0 kcal/mol (***Du-GC***) were obtained, which were enthalpic driven, -51.0 kcal/mol for both duplexes. These folding enthalpies were in excellent agreement with nearest-neighbor enthalpies (-51.4 and -50.6 kcal/mol, respectively) [**38**]. In 5 M salt, the Δ*G*° terms were less favorable (by 1.4 and 1.9 kcal/mol, respectively), while the enthalpy terms were slightly lowered by 1.9 kcal/mol (***Du-CG***) and 2.7 kcal/mol (***Du-GC***). Furthermore, we used these thermodynamic profiles to estimate thermodynamic parameters for the following hypothetical reaction: ***Du-CG*** → ***Du-GC***, which assumed that the single strands were similar at high temperatures. Therefore, the thermodynamic profiles for the folding of ***Du-CG*** were subtracted from the profiles of ***Du-GC***. This exercise yielded a ΔΔ*H* = -0.3 kcal/mol, with a ΔΔ*G*° of 0.3 kcal/mol in 1 M NaCl and ΔΔ*H* of -1.1 kcal/mol, with a ΔΔ*G*° of -0.2 kcal/mol in 5 M. This showed that there is little to no thermodynamic effect on the conversion of the helix from left handed to right headed.

The analysis of the pseudoknot data in 1 M NaCl (**Table 1**), and using similar hypothetical thermodynamic cycles, indicated the folding of ***GC-PsK*** was entropically, (Δ(TΔ*S*)=9.1 kcal/mol) more stable than ***CG-PsK*** by $\Delta\Delta G^\circ_{20}$=-1.1 kcal/mol; while in 5 M, ***CG-PsK*** was entropically (Δ(TΔ*S*)=16.8 kcal/mol) more stable than ***GC-PsK*** by $\Delta\Delta G^\circ_{20}$=-1.2 kcal/mol. In the following paragraph, we have analyzed each of the two motifs in the pseudoknots in a similar way.

The thermodynamic comparison of the second and third transition of ***CG-PsK*** and ***GC-PsK***, respectively, produced the effect of the presence of the GC rich domain within the pseudoknot. In 1 M NaCl, ***GC-PsK*** had a more favorable Δ*G*° of -0.9 kcal/mol and more favorable Δ*H* of -1.6 kcal, while in 5 M NaCl, ***CG-PSK*** had a more favorable Δ*G*° of -0.4 kcal/mol and more favorable Δ*H* of -3.3 kcal/mol. Both sets were very similar to the comparative data of the control duplexes. This indicated that the inclusion of this GC rich motif in the pseudoknot does not affect its overall thermodynamic profiles, even if the d(CGCGCG)$_2$ undergoes a conformational change to a left handed helix in 5 M NaCl. This observation was consistent with the zeroth energy change for the helical transition of a right to left handed helix [**40**]. This also showed that once the bottom strand is melted, there was no strain on the left stem. Therefore, the left stem in either pseudoknot was able to unfold similar to the corresponding duplex.

The comparison of the thermodynamic parameters of the first transition of ***CG-PsK*** with those of the initial two transitions of ***GC-PsK*** yielded the melting behavior of the AT rich domain i.e., the right stem of the pseudoknots. In 1 M NaCl, ***GC-PsK*** was more stable, by ΔΔ*G*°=-0.2 kcal/mol and had a less favorable ΔΔ*H* of 9.6 kcal/mol. In 5 M NaCl, ***GC-PsK*** was less stable, by a Δ*G*°=0.8 kcal/mol with a less favorable ΔΔ*H* of 14.7 kcal/mol. However, the GA/CT and TC/AG base pair stacks of ***CG-PsK*** and CA/GT and TG/AC stacks of ***GC-PsK*** only differed by 0.6 kcal/mol. This indicated that the large difference in the folding enthalpies of these pseudoknots was due to an interplay of the right stem of the pseudoknots with its loop; the stem base pairs may be weakened by the presence of the adjacent loop of 5 thymines that can be partially complementary to four bases on the stem, 3 adenines and 1 guanine. For instance, the differences between the two stems were the bases in the 7th position of the stem, G in ***GC-PsK*** and C in ***CG-PsK***, and the 13th position of the stem, C in ***GC-PsK*** and G in ***CG-PsK***; each guanine could be in a wobble dG•dT base pair with the first and last thymine of the loop in ***GC-PsK*** and ***CG-PsK***., respectively, creating additional constrain because each loop would now have only four thymines. Most likely a dG•dT base pair would form in ***GC-PsK*** and not in ***CG-PsK*** because the two bases are adjacent. In addition, three loop thymines could form three dT*dA•dT base triplets, but this is unlikely because the folding enthalpy would be much higher. The main observation was this loop/stem interplay could form loose base pair stacks in the right stem of ***GC-PsK***, yielding a lower folding enthalpy for this pseudoknot in 1 & 5 M NaCl. Furthermore, the lower enthalpy of ***GC-PsK*** obtained in 5 M, compared to ***CG-PsK***, may be explained in terms of the lowered hydration of the AT base pairs of this motif (41) and/or the formation of the left handed helix in the native form of ***CG-PsK*** may be lowering the interplay of the loop with the stem; thus, lowering the overall loop/stem constrain.

Conclusions

We have investigated the thermodynamic stability of two pseudoknots. Specifically, we used a combination of UV, CD, and DSC techniques to determine the unfolding thermodynamics of a pair of pseudoknots and their control duplexes. The favorable folding of DNA pseudoknots resulted from the typical favorable enthalpy-unfavorable entropy compensation; enthalpy contributions corresponded to formation of

doi: 10.7243/2052-9341-5-4

base pair stacks while the entropy contributions were due to the ordering of the oligonucleotides and uptake of ions and water. This confirmed the flexibility of DNA strands being able to form pseudoknots that can be used to mimic known RNA secondary structures. The UV and DSC unfolding curves showed biphasic (***CG-PsK***) and biphasic/triphasic (***GC-PsK***) transitions, respectively, with T_Ms independent on the strand concentration, i.e., each pseudoknot unfolds intramolecularly. All transitions were sequential and correspond to the associated melting domains. In addition, the placement of the d(CGCGCG) in ***CG-PsK*** formed a left-handed helix in 5 M NaCl. Overall, ***CG^{2}PsK*** unfolded in two transitions corresponding to the AT and GC rich stem motifs of the pseudoknot. The salt concentration did not significantly affect the overall thermodynamics of this pseudoknot. ***GC-PsK*** unfolded in three transitions with the first two corresponding to the AT rich stem and the last transition being the GC rich stem. However, the folding enthalpy of this pseudoknot was affected by the increase in salt concentration from 1 M to 5 M. The differences in the melting behavior of these pseudoknots, especially the AT rich motif, can be explained in terms of the loop/stem interplay within the ***GC-PsK*** pseudoknot, hydration differences of their dA•dT base pairs, and/or the conversion of ***CG-PsK*** to a partial left handed helix. This conversion could be helping to stabilize this pseudoknot allowing the right stem to be less constrained at 5 M NaCl.

Competing interests

The authors declare that they have no competing interests.

Authors' contributions

Authors' contributions	CS	MN	LAM
Research concept and design	--	--	✓
Collection and/or assembly of data	✓	✓	✓
Data analysis and interpretation	✓	✓	✓
Writing the article	✓	--	✓
Critical revision of the article	✓	--	✓
Final approval of article	✓	--	✓
Statistical analysis	--	--	--

Acknowledgements

This work was supported by National Science Foundation Grant MCB-1122029.

Publication history

Editor: Mariusz Skwarczynski, University of Queensland, Australia.
Received: 30-Mar-2017 Final Revised: 08-Jun-2017
Accepted: 29-Jun-2017 Published: 13-Jul-2017

References

1. Wang AH, Quigley GJ, Kolpak FJ, Crawford JL, van Boom JH, van der Marel G and Rich A. **Molecular structure of a left-handed double helical DNA fragment at atomic resolution**. *Nature*. 1979; **282**:680-6. | PubMed
2. Rich A and Zhang S. **Timeline: Z-DNA: the long road to biological function**. *Nat Rev Genet*. 2003; **4**:566-72. | Article | PubMed
3. Thamann TJ, Lord RC, Wang AH and Rich A. **The high salt form of poly(dG-dC).poly(dG-dC) is left-handed Z-DNA: Raman spectra of crystals and solutions**. *Nucleic Acids Res*. 1981; **9**:5443-57. | PubMed Abstract | PubMed FullText
4. Pohl FM and Jovin TM. **Salt-induced co-operative conformational change of a synthetic DNA: equilibrium and kinetic studies with poly (dG-dC)**. *J Mol Biol*. 1972; **67**:375-96. | Article | PubMed
5. Behe M and Felsenfeld G. **Effects of methylation on a synthetic polynucleotide: the B--Z transition in poly(dG-m5dC).poly(dG-m5dC)**. *Proc Natl Acad Sci U S A*. 1981; **78**:1619-23. | PubMed Abstract | PubMed FullText
6. Zacharias W, Jaworski A and Wells RD. **Cytosine methylation enhances Z-DNA formation in vivo**. *J Bacteriol*. 1990; **172**:3278-83. | Article | PubMed Abstract | PubMed FullText
7. Peck LJ, Nordheim A, Rich A and Wang JC. **Flipping of cloned d(pCpG) n.d(pCpG)n DNA sequences from right- to left-handed helical structure by salt, Co(III), or negative supercoiling**. *Proc Natl Acad Sci U S A*. 1982; **79**:4560-4. | Pdf | PubMed Abstract | PubMed FullText
8. Schroth GP, Chou PJ and Ho PS. **Mapping Z-DNA in the human genome. Computer-aided mapping reveals a nonrandom distribution of potential Z-DNA-forming sequences in human genes**. *J Biol Chem*. 1992; **267**:11846-55. | Article | PubMed
9. Liu LF and Wang JC. **Supercoiling of the DNA template during transcription**. *Proc Natl Acad Sci U S A*. 1987; **84**:7024-7. | Article | PubMed Abstract | PubMed FullText
10. Wittig B, Dorbic T and Rich A. **The level of Z-DNA in metabolically active, permeabilized mammalian cell nuclei is regulated by torsional strain**. *J Cell Biol*. 1989; **108**:755-64. | Article | PubMed Abstract | PubMed FullText
11. Herbert A and Rich A. **The biology of left-handed Z-DNA**. *J Biol Chem*. 1996; **271**:11595-8. | Article | PubMed
12. Rahmouni AR and Wells RD. **Stabilization of Z DNA in vivo by localized supercoiling**. *Science*. 1989; **246**:358-63. | Article | PubMed
13. Jaworski A, Higgins NP, Wells RD and Zacharias W. **Topoisomerase mutants and physiological conditions control supercoiling and Z-DNA formation in vivo**. *J Biol Chem*. 1991; **266**:2576-81. | Article | PubMed
14. Lafer EM, Moller A, Nordheim A, Stollar BD and Rich A. **Antibodies specific for left-handed Z-DNA**. *Proc Natl Acad Sci U S A*. 1981; **78**:3546-50. | PubMed Abstract | PubMed FullText
15. Moller A, Gabriels JE, Lafer EM, Nordheim A, Rich A and Stollar BD. **Monoclonal antibodies recognize different parts of Z-DNA**. *J Biol Chem*. 1982; **257**:12081-5. | Article | PubMed
16. Herbert A and Rich A. **The role of binding domains for dsRNA and Z-DNA in the in vivo editing of minimal substrates by ADAR1**. *Proc Natl Acad Sci U S A*. 2001; **98**:12132-7. | Article | PubMed Abstract | PubMed FullText
17. Kim YG, Muralinath M, Brandt T, Pearcy M, Hauns K, Lowenhaupt K, Jacobs BL and Rich A. **A role for Z-DNA binding in vaccinia virus pathogenesis**. *Proc Natl Acad Sci U S A*. 2003; **100**:6974-9. | Article | PubMed Abstract | PubMed FullText
18. Wittig B, Dorbic T and Rich A. **The level of Z-DNA in metabolically active, permeabilized mammalian cell nuclei is regulated by torsional strain**. *J Cell Biol*. 1989; **108**:755-64. | Article | PubMed Abstract | PubMed FullText
19. Wittig B, Dorbic T and Rich A. **Transcription is associated with Z-DNA formation in metabolically active permeabilized mammalian cell nuclei**. *Proc Natl Acad Sci U S A*. 1991; **88**:2259-63. | Article | PubMed Abstract | PubMed FullText
20. Isambert H and Siggia ED. **Modeling RNA folding paths with pseudoknots: application to hepatitis delta virus ribozyme**. *Proc Natl Acad Sci U S A*. 2000; **97**:6515-20. | Article | PubMed Abstract | PubMed FullText
21. Ke A, Zhou K, Ding F, Cate JH and Doudna JA. **A conformational switch controls hepatitis delta virus ribozyme catalysis**. *Nature*. 2004; **429**:201-5. | Article | PubMed
22. Adams PL, Stahley MR, Kosek AB, Wang J and Strobel SA. **Crystal structure of a self-splicing group I intron with both exons**. *Nature*. 2004; **430**:45-50. | Article | PubMed
23. Souliere MF, Altman RB, Schwarz V, Haller A, Blanchard SC and Micura

doi: 10.7243/2052-9341-5-4

R. **Tuning a riboswitch response through structural extension of a pseudoknot**. *Proc Natl Acad Sci U S A*. 2013; **110**:E3256-64. | Article | PubMed Abstract | PubMed FullText

24. Chen G, Chang KY, Chou MY, Bustamante C and Tinoco I Jr. **Triplex structures in an RNA pseudoknot enhance mechanical stability and increase effieciency of -1 ribosomal frameshifting**. *PNAS*. 2009; **106**:12706–12711.
25. Teng MK, Liaw YC, van der Marel GA, van Boom JH and Wang AH. **Effects of the O2' hydroxyl group on Z-DNA conformation: structure of Z-RNA and (araC)-[Z-DNA]**. *Biochemistry*. 1989; **28**:4923-8. | PubMed
26. Davis PW, Adamiak RW and Tinoco I, Jr. **Z-RNA: the solution NMR structure of r(CGCGCG)**. *Biopolymers*. 1990; **29**:109-22. | Article | PubMed
27. Liberman JA, Salim M, Krucinska J and Wedekind JE. **Structure of a class II preQ1 riboswitch reveals ligand recognition by a new fold**. *Nat Chem Biol*. 2013; **9**:353-5. | Article | PubMed Abstract | PubMed FullText
28. McCown PJ, Liang JJ, Weinberg Z and Breaker RR. **Structural, functional, and taxonomic diversity of three preQ1 riboswitch classes**. *Chem Biol*. 2014; **21**:880-9. | Article | PubMed Abstract | PubMed FullText
29. Cantor CR, Warshaw MM and Shapiro H. **Oligonucleotide interactions. 3. Circular dichroism studies of the conformation of deoxyoligonucleotides**. *Biopolymers*. 1970; **9**:1059-77. | Article | PubMed
30. Marky LA and Breslauer KJ. **Calculating thermodynamic data for transitions of any molecularity from equilibrium melting curves**. *Biopolymers*. 1987; **26**:1601-20. | Article | PubMed
31. Marky LA, Maiti S, Olsen CM, Shikiya R, Johnson SE, Kaushik M and Khutsishvili I. **Building blocks of nucleic acid nanostructures: unfolding thermodynamics of intramolecular DNA complexes**. in: V. Labhasetwar, D. Leslie-Pelecky (Eds.), *Biomedical Applications of Nanotechnology, John Wiley & Sons, Inc.* 2007; 191-225.
32. Miyahara T, Nakatsuji H and Sugiyama H. **Helical structure and circular dichroism spectra of DNA: a theoretical study**. *J Phys Chem A*. 2013; **117**:42-55. | Article | PubMed
33. Kypr J, Kejnovska I, Renciuk D and Vorlickova M. **Circular dichroism and conformational polymorphism of DNA**. *Nucleic Acids Res*. 2009; **37**:1713-25. | Article | PubMed Abstract | PubMed FullText
34. Olsen CM, Shikiya R, Ganugula R, Reiling-Steffensmeier C, Khutsishvili I, Johnson SE and Marky LA. **Application of differential scanning calorimetry to measure the differential binding of ions, water and protons in the unfolding of DNA molecules**. *Biochim Biophys Acta*. 2016; **1860**:990-8. | Article | PubMed
35. Prislan I, Lee H-T, Lee C and Marky LA. **The Size of Internal Loops Influences the Unfolding Thermodynamics of DNA Hairpins**. In ACS Symposium Series 1082. Frontiers in Nucleic Acids, R. D. Sheardy and S. A. Winkle, Editors, 2011; 93-110.
36. Lee HT, Khutsishvili I and Marky LA. **DNA complexes containing joined triplex and duplex motifs: melting behavior of intramolecular and bimolecular complexes with similar sequences**. *J Phys Chem B*. 2010; **114**:541-8. | Article | PubMed
37. Olsen CM and Marky LA. **Energetic and hydration contributions of the removal of methyl groups from thymine to form uracil in G-quadruplexes**. *J Phys Chem B*. 2009; **113**:9-11. | PubMed
38. SantaLucia J, Jr. **A unified view of polymer, dumbbell, and oligonucleotide DNA nearest-neighbor thermodynamics**. *Proc Natl Acad Sci U S A*. 1998; **95**:1460-5. | Article | PubMed Abstract | PubMed FullText
39. Reiling C, Khutsishvili I, Huang K and Marky LA. **Loop contributions to the folding thermodynamics of DNA straight hairpin loops and pseudoknots**. *J Phys Chem B*. 2015; **119**:1939-46. | Article | PubMed
40. Peck LJ and Wang JC. **Energetics of B-to-Z transition in DNA**. *Proc Natl Acad Sci U S A*. 1983; **80**:6206-10. | Article | PubMed Abstract | PubMed FullText
41. Schorschinsky N and Behe MJ. **The B-Z transition of a polynucleotide with a 10-base pair repeating sequence**. *J Biol Chem*. 1986; **261**:8093-5. | Article | PubMed

Citation:
Reiling-Steffensmeier C, Nordeen M and Marky LA. **Melting behavior of pseudoknots containing adjacent GC and AT rich domains**. *Bio Chem Comp*. 2017; **5**:4.
http://dx.doi.org/10.7243/2052-9341-5-4